World Journal of Advanced Engineering Technology and Sciences
eISSN: 2582-8266
Cross Ref DOI: 10.30574/wjaets
Journal homepage: https://wjaets.com/

(RESEARCH ARTICLE)

Check for updates

Integrating GIS and remote sensing in mapping soil erosion risk using SLEMSA model: A case study of Dinogeng Agricultural Extension Area of Kgatleng District, Botswana

Lucky Sitayelo [1], Benedict Kayombo [1,*], Cecil Patrick [1] and Ednah Kgosiesele [2]

[1] *Department of Agricultural and Biosystems Engineering, Botswana University of Agriculture and Natural Resources, Private Bag 0027, Gaborone, Botswana.*
[2] *Department of Wildlife and Aquatic Resources, Botswana University of Agriculture and Natural Resources, Private Bag 0027, Gaborone, Botswana.*

World Journal of Advanced Engineering Technology and Sciences, 2022, 07(02), 001–012

Publication history: Received on 22 August 2022; revised on 24 October 2022; accepted on 27 October 2022

Article DOI: https://doi.org/10.30574/wjaets.2022.7.2.0111

Abstract

A study was conducted in Dinogeng Agricultural Extension Area (DAEA) of Kgatleng District, Botswana, with the objective of assessing current soil erosion risk (using 2020 Landsat imagery) resulting from the Integrated Support Programme for Arable Agricultural Development (ISPAAD) that was launched in 2009. The Soil Loss Estimation Model for Southern Africa (SLEMSA) tool integrated with Geographical Information System (GIS) and Remote Sensing assessed the soil erosion risk in the study area. The results indicated that 88% of DAEA has low to moderate soil erosion risk (0 – 2 $tha^{-1}yr^{-1}$). Only 12% of the study area experience very high to extreme high erosion risk (5 - ≥10 $tha^{-1}yr^{-1}$) along the streams, at steep slopes and areas of bare land. Common practice calls for conservation measures to be applied on areas with high soil loss. This study has underscored the role of topography and soil erodibility, as natural factors, in driving soil erosion.

Keywords: DAEA; ISPAAD; SLEMSA; Soil erosion risk

1. Introduction

Soil erosion is one of the major worldwide environmental hazards causing severe land degradation. The estimated mean rates of soil erosion across the world ranges between 12 and 15 t ha^{-1} yr^{-1} [1]. In the Ethiopian highlands, an annual soil loss reaches 200-300 tons ha^{-1} $year^{-1}$ [2]. Botswana, located in semi-arid environments, is most vulnerable to soil erosion threats due to less biomass to sustain soil structural integrity [3]. Population explosion, deforestation, unsustainable agricultural cultivation, and overgrazing are among the main factors causing soil erosion hazards. A study by Kayombo et al. [4] observed that the deterioration of soil quality, in terms of nutrient depletion and poor physical properties for cultivated as compared to virgin soils was a result of continuous cultivation. The average crop yield from a piece of land in Botswana is very low mainly due to soil fertility decline associated with removal of topsoil by erosion.

Soil loss risk can now be estimated from a wide range of empirical, conceptual and physical based models [5, 6]. These models vary in complexity, data requirements, processes and calibration, and include statistical model of the Universal Soil Loss Equation (USLE) and its derivatives - Revised Universal Soil Loss Equation (RUSLE), Soil Loss Estimation Model for Southern Africa (SLEMSA), and Soil and Water Assessment Tool (SWAT) or the Water Erosion Prediction Project (WEPP). In general, model selection is particularly dependent on the availability of data, attributes of a working area and intended use. The dominant model adopted in most countries in Southern Africa and selected for this study is the SLEMSA model.

* Corresponding author: Benedict Kayombo
Department of Agricultural and Biosystems Engineering, Botswana University of Agriculture and Natural Resources, Private Bag 0027, Gaborone, Botswana.

Introduction of Geographical Information Systems (GIS) and Remote Sensing (RS) technology has made it possible to implement the equation in a spatially distributed manner and prediction of soil erosion on a cell-by-cell basis using the SLEMSA model [7].

Several studies have been carried out by different researchers on soil erosion risk modelling. However, the implementation of SLEMSA model has received little attention in Botswana. Less is known about the spatial extent and distribution within human-induced disturbed areas at an agricultural extension area scale. The objective of the present study was, therefore, to model soil erosion in the Dinogeng Agricultural Extension Area of Kgatleng District using SLEMSA integrated with GIS and Remote Sensing.

2. Material and methods

2.1. Study site description

The study area extends from 24^0 8 0' to 24^0 35 0' S latitude and 26^0 5 0' to 26^0 35 0' E longitude and it covers an area of about 83 100 hectares. The climate is semiarid with a mean annual average temperature of 20.7 ^{0}C fluctuating from 13.2 °C to 28.2 °C. The topography is flat and undulating, with the elevation ranging from 901 to 1003m. The communities in the study area depend on ground water for their livelihood. The soils are predominantly Luvisols with a textural inclination from sandy clay loam to sandy clay. The vegetation of the study site is dominated by shrubs with areas of woodland and savanna. Almost 50% of the area is covered by shrubs; about 7% is evergreen forest mainly along the Notwane River and other drainage lines (Sitayelo, 2022). An overview of the boundary of the study area is given in Figure 1.

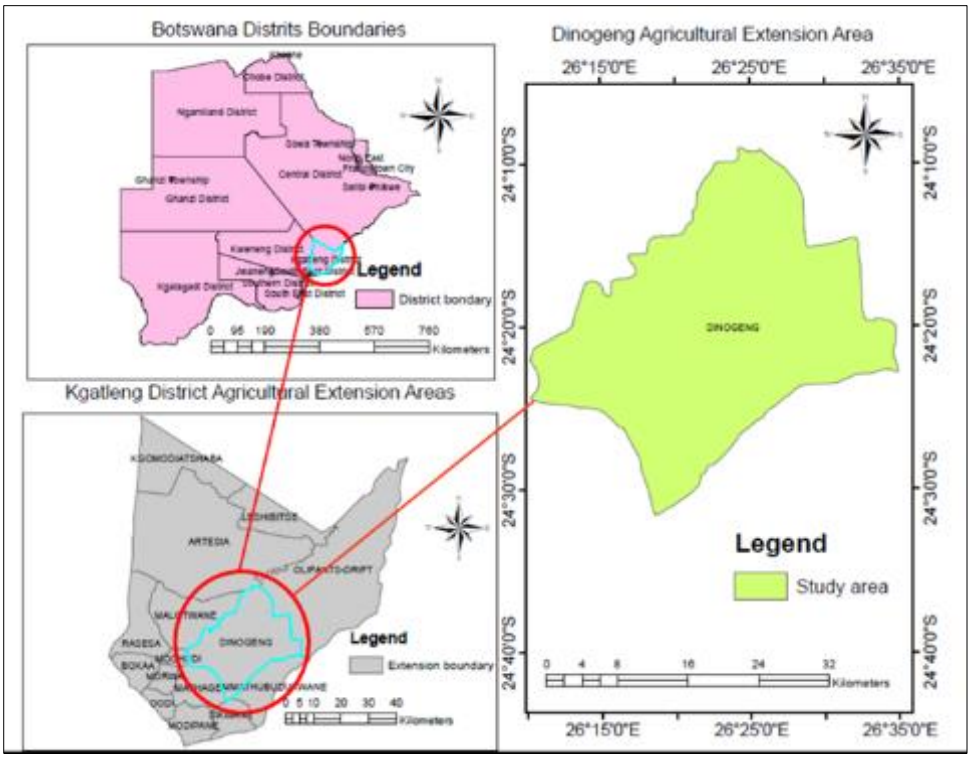

Figure 1 Location of Dinogeng within Kgatleng District in Botswana

2.2. Mapping of soil erosion risk

Mapping of soil erosion risk in the study area was carried out according to SLEMSA model. The model input data included rainfall energy, soil erodibility, slopes length and steepness, topographic factor, crop ratio and principal factor.

2.2.1. Rainfall Energy (E)

The monthly rainfall amounts of Dinogeng were collected for over 19 years from the Department of Meteorological Services (DMS). Monthly rainfall records from three nearby meteorological stations covering various periods between

1995 and 2019 were used to calculate the mean annual rainfall. Rainfall energy was then determined according to Equation (1) for erosive rainfall [8, 9]. The mean annual rainfall was first interpolated to generate continuous rainfall data for each grid cell by using Analyst Tools Raster Inverse Distance Weighting (IDW) Interpolation in ArcGIS to create a raster map for the area shown in Figure 2. The rainfall stations were selected based on the availability of complete data and their proximity to the study area. Details of the rainfall stations are presented in Table 1

$$E = 18.846*MAP \quad \text{..... (1)}$$

Where, E is the rainfall energy and MAP is the mean annual precipitation (mm).

Table 1 Meteorological variable records for the stations

Station no.	Station ID	Station name	Latitude °S	Longitude °E	Elevation amsl (m)	Average Annual Rainfall mm	Period
1	136	Mochudi Police	24⁰ 23’	26⁰ 8’	945	405	2000 to 2019
2	177	Olifantsdrift Police	24⁰ 12’	26⁰ 41’	855	326	1995 to 2019
3	228	Sikwane Police	24⁰ 25’	26⁰ 27’	915	373	1995 to 2019

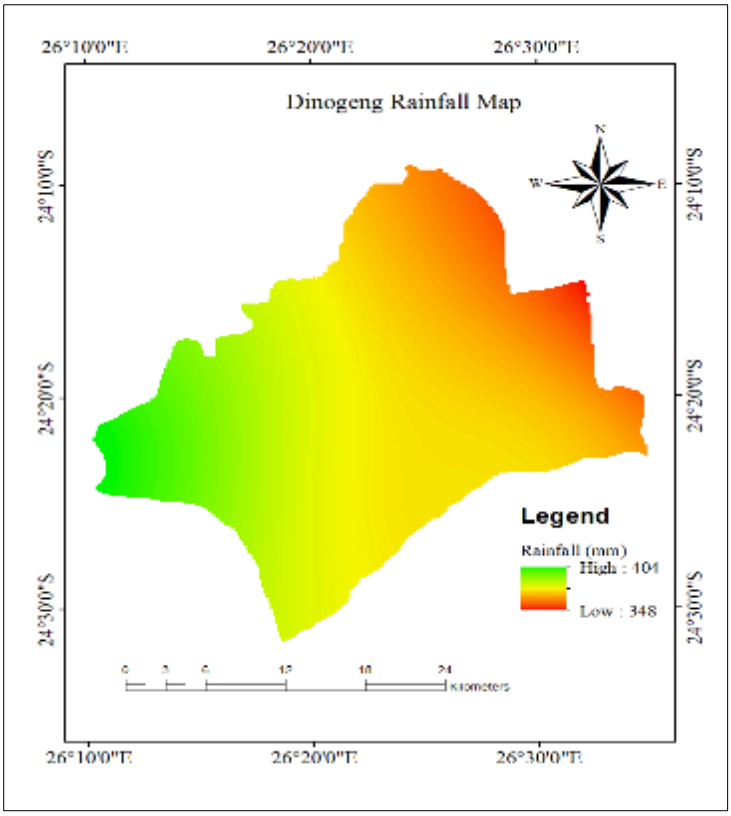

Figure 2 Dinogeng spatial rainfall variability

2.2.2. Soil Erodibility Factor (F)

The soil units’ map for the area of interest was extracted from Kgatleng District digital soil map at 1: 250 000 scale by masking using Spatial Analyst Tools within ArcGIS environment. The soil erodibility (F) factor given in Table 2 was estimated based on local condition and soil texture [2, 5, 7, 10, 11]. The F value increased with declining probability of soil erodibility. The resulting shape file was converted to raster format with a cell size of 30 m x 30 m. The raster map was then reclassified based on their erodibility values.

Table 2 Soil erodibility factor (F) values

Soil texture	Soil type	F value
Light	Sands, Loamy sands, Sandy Loams	4
Medium	Sandy clay Loam, Sandy clay	5
Heavy	Clay, Heavy clay	6

2.2.3. Slope length and slope steepness

The Shuttle Radar Topography Mission (SRTM) Digital Elevation Model (DEM) of spatial resolution of 30 m was used to generate slope using Spatial Analyst Tools within ArcMap 10.7 environment. Flow accumulation and slope steepness were then calculated using filled DEM with a Raster Calculator in ArcGIS [2], using Equations (2) and (3):

$$l = \text{Flow accumulation} * \text{cell size} \quad \text{(2)}$$

$$S = (0.43 + 0.30\,s + 0.043\,s^2)/6.613 \quad \text{(3)}$$

Where;
l is the slope length,
S is the slope gradient factor and s is the gradient (%).

2.2.4. Topographic factor (X)

The topographic ratio is a product of two factors: a slope gradient factor and a slope length factor. The slope length and slope gradient factors were calculated using the filled DEM and entered the Equation (4) [12] to produce the topographic factor grid map. To calculate the slope length, derivation of flow accumulation was based on the DEM after conducting the Fill and Flow direction process respectively in ArcGIS [13].

$$X = \sqrt{(l/22.1)}\,(0.065 + 0.045S + 0.0065S^2) \quad \text{(4)}$$

Where;
X is the topographic ratio,
l is the slope length (m), S is slope (%).

2.2.5. Crop ratio (C)

The land cover classification generated from Landsat 8 imagery for the year 2020 was used to determine the C-factor. Due to the lack of detailed information and difficulties in processing, C-factor values were assigned to every class in a GIS using a raster calculator, based on literature data in Table 3.

Table 3 C-factor values for the study area

No	Land cover classes	C-factor values	Source
1	Shrub	0.014	[11]
2	Forest	0.01	[14]
3	Cultivated land	0.15	[2]
4	Bare land	0.6	[13, 14]

2.2.6. Principal factor (K)

The value of the K factor was determined by relating mean annual soil loss to mean annual rainfall energy (E) using Equation (5) [15]

$$\ln K = b \ln E + a \quad \text{Equation (5)}$$

Where;

E is in $Jm^{-2}mm^{-1}$;
a and b are functions of the soil erodibility factor (*F*):

$$a = 2.884 - 8.2109F \quad \text{(6)}$$

$$b = 0.4681 + 0.7663F \quad \text{(7)}$$

Equations (6) and (7) were substituted into equation (5) to get the final Equation (8) used for estimation of the K factor.

$$K = \exp[(0.4681 + 0.7663*(F)) \ln E + 2.884 + (8.1209*F)] \quad \text{(8)}$$

K factor values were assigned to respective soil types in soil map to generate the soil erodibility map using GIS.

2.2.7. Soil loss analysis

The overall procedure involved the use of the SLEMSA model in a GIS environment. The input parameters obtained from meteorological stations, soil map, topographic map, satellite images and DEM were processed as shown in Figure 3. A cell-by-cell analysis of the soil loss was done to determine annual soil loss rate by overlaying and multiplying the respective SLEMSA sub-model values (*K, C,* and *X*) interactively by using Spatial Analyst Tool Map Algebra Raster Calculator in ArcGIS 10.7 environment as shown in Equation (9).

$$Z = KCX \ [8] \quad \text{(9)}$$

Where;
Z is the predicted mean annual soil loss in $tha^{-1}yr^{-1}$;
K is the mean annual soil loss in $tha^{-1}yr^{-1}$ from a standard field plot 30 x 10 m with a slope of 4.5% and for a soil of a known erodibility rating *F* under a weed-free bare fallow;
C is the ratio of soil lost from a cropped plot to that lost from bare fallow;
X is the ratio to account for different slope steepness and length.

The soil loss potential was then categorized into different severity classes to determine erosion risk priority areas for conservation planning [6].

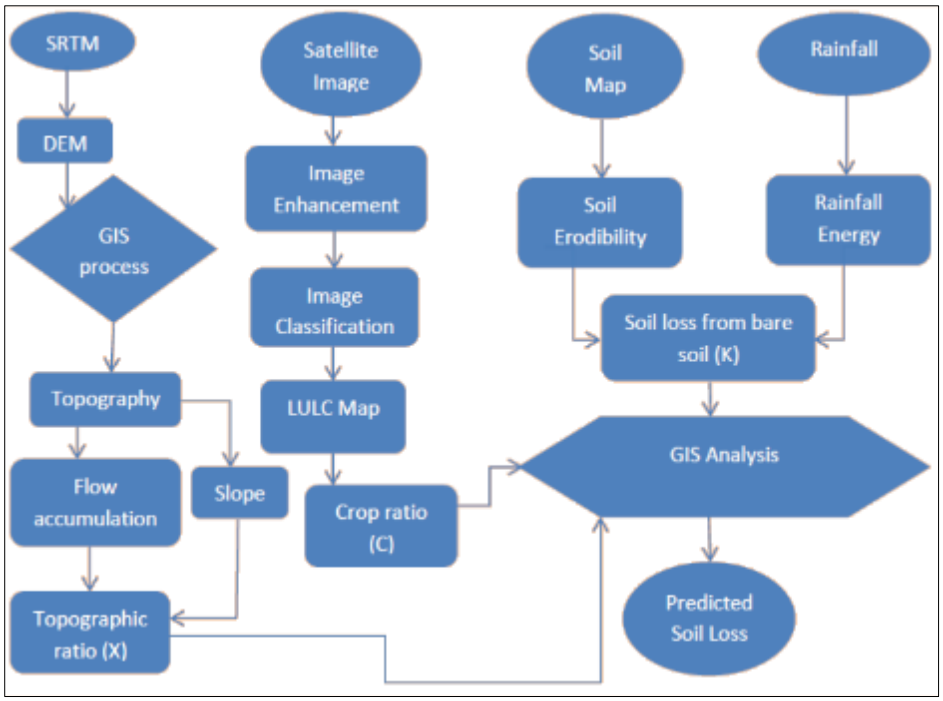

Figure 3 Flowchart for implementation of SLEMSA model

2.3. Software Packages and Data Processing

Geomatica 2018 Catalyst Professional software was used for image processing and digital image classification or spectral class recognition was accomplished by supervised classification. The classification results (i.e. land cover raster image) were exported into ArcMap 10.7 for accuracy assessment with the aid of high-resolution imagery software, Google Earth and Google Earth Pro. Layers were spatially organized with the same resolution and coordinate system within ArcGIS environment [16]. Microsoft Office was used for presentation, documentation and pre-processing calculations in excel environment. The GeoConverter-Geoplaner software package was used for converting geographical coordinates.

3. Results and discussion

3.1. Mapping of soil erosion risk

Mapping of soil erosion in the study area was carried out according to SLEMSA model. The SLEMSA model includes topographic indices derived from the DEM, climatic factors, vegetation and soil characteristics.

3.1.1. Topographic Ratio (X)

The DEM, slope and flow accumulation maps are presented in Figure 4. The input factors were combined to determine the topographic factor map (Figure 5) using Equation (4). The topographic ratio ranged from 0 to a maximum of 41.2 as observed in Figure 4. The findings show that the slope and flow accumulation are heavily influenced by altitude and by increasing their values, the topographic ratio factor also implies an increasing trend.

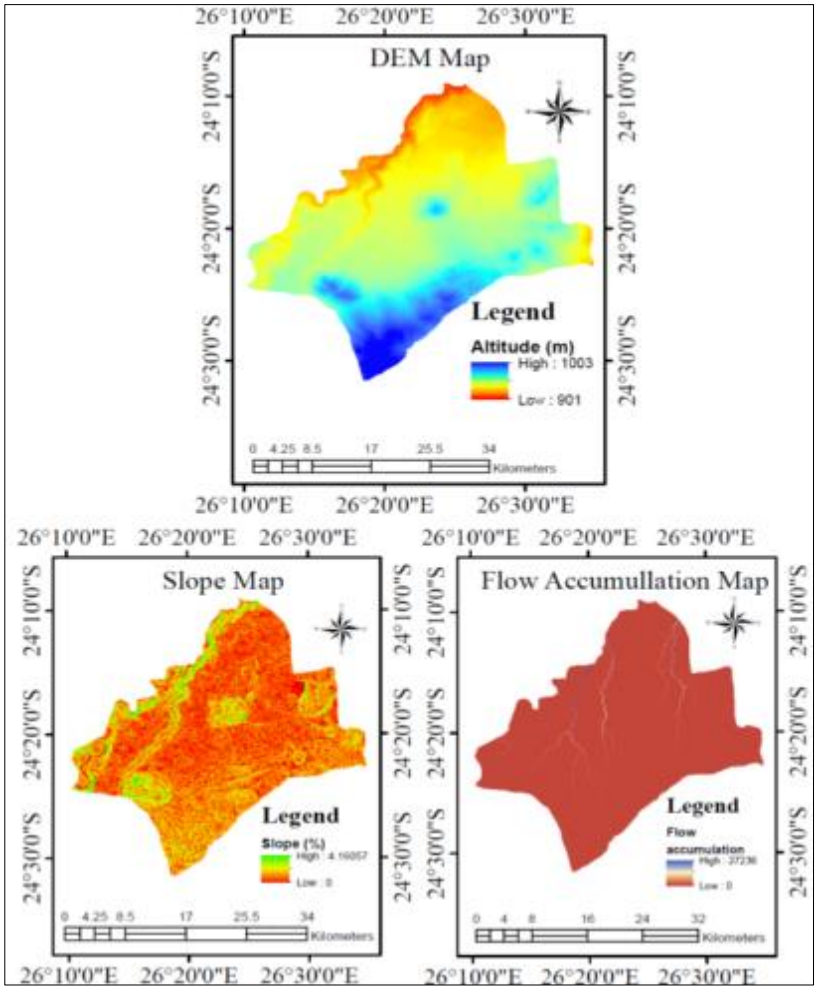

Figure 4 Topographic Ratio input factors and DEM

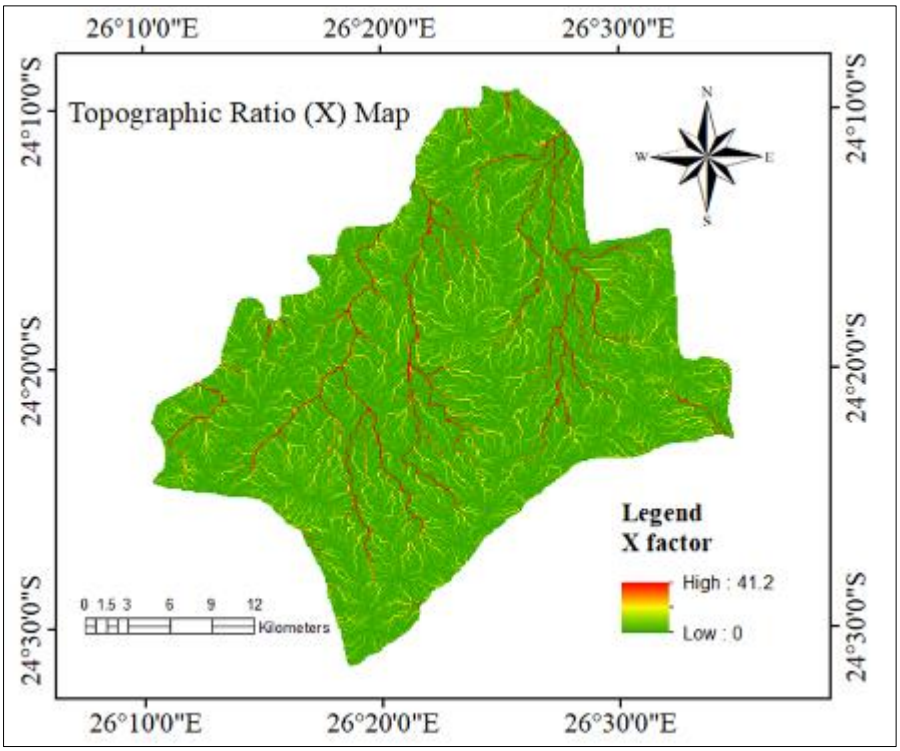

Figure 5 Topographic ratio (X factor) map

3.1.2. Rainfall energy (E)

The mean annual precipitation data interpolated over the entire study area using IDW interpolation technique was converted to rainfall energy by applying Equation (1). The annual rainfall of Dinogeng ranges from 347.8 mm to 403.9mm. The result showed that the average E factor value in the study area was 7071 MJmmha^{-1} year^{-1} ranging from 6554MJmmha^{-1} to 7612 MJmmha^{-1} as shown in Figure 6.

3.1.3. Soil erodibility factor (F)

Soils which are highly susceptible to erosion have erodibility values close to 1, whereas corresponding values close to 10 indicate the resistive nature of the soil as shown in Figure 6. In the current study, information on soil structure and profile permeability was not available. Therefore, the F factor was appraised based on soil texture as shown in Table 4.

Table 4 Method of assessing F value (Heydarnejad et al., 2020)

Soil texture	Soil type	F value
Light	Sands, Loamy sands, Sandy Loams	4
Medium	Sandy clay Loam, Sandy clay	5
Heavy	Clay, Heavy clay	6

3.1.4. Principal factor (K)

After determining the values of F and E, the value of K was calculated using Equation (8) in a GIS environment to produce a map. The results show that the K factor ranges between 1.1 tha^{-1}yr^{-1} and 7.2 tha^{-1}yr^{-1} (Figure 6) with an average value of 2.5 tha^{-1}yr^{-1}.

3.1.5. Crop ratio factor (C)

To evaluate and determine the crop ratio, indicating the amount of soil loss at bare surfaces and the effect of vegetation on soil conservation, C-factor values were assigned to every LULC class in a GIS using a raster calculator, based on literature data in Table 5 and the values ranged from 0.01 to 0.6 as shown in Figure 7.

Table 5 C-factor values for the study area

No	Land cover classes	C-factor values	Source
1	Shrub	0.014	[11]
2	Forest	0.01	[14]
3	Cultivated land	0.15	[2]
4	Bare land	0.6	[13, 14]

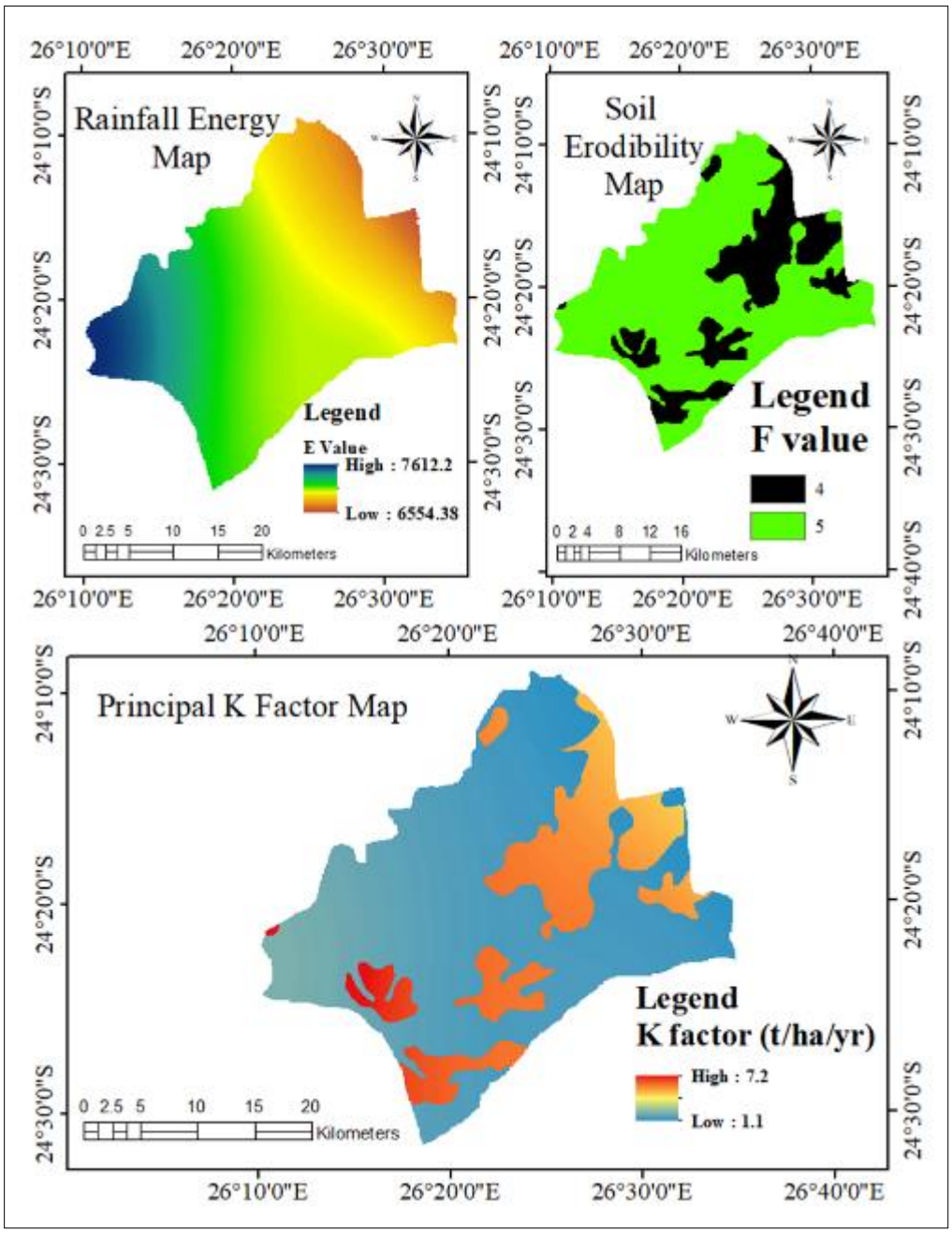

Figure 6 Principal K and input factors

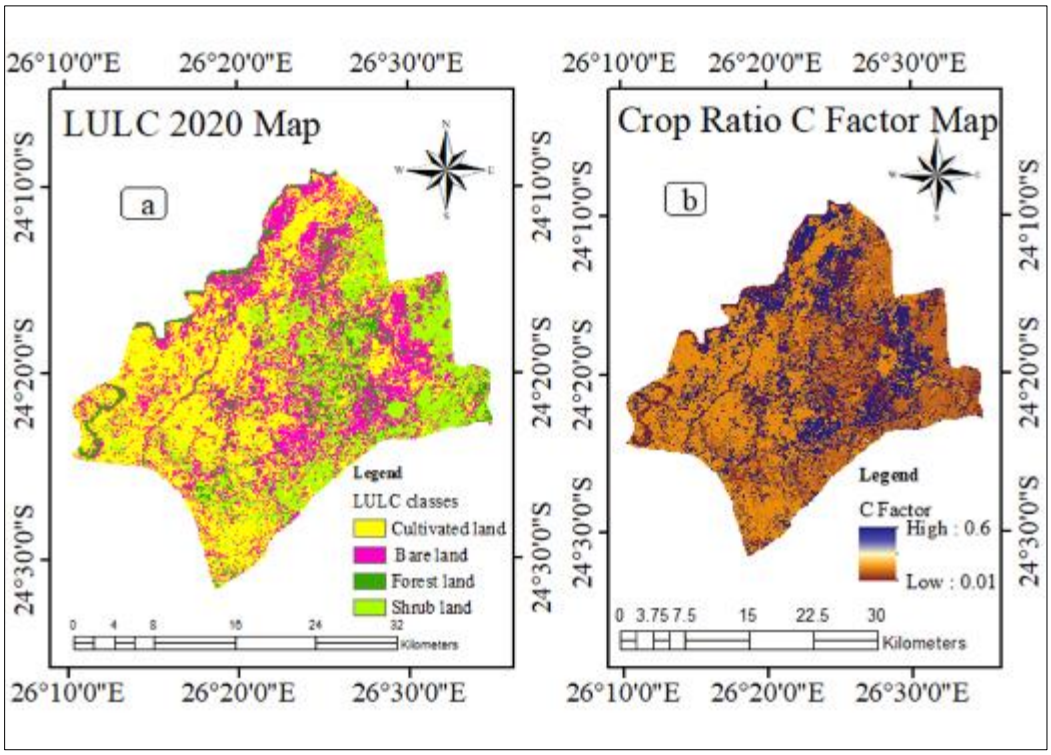

Figure 7 Spatial distribution of (a) LULC for 2020 and (b) Crop ratio

3.2. Determination of SLEMSA model (Z)

The calculation of erosion in this model was carried out through equation Z = KCX (Elwell, 1978) to obtain the annual soil loss map shown in Figure 8. The results were then used to determine different categories of erosion risk areas shown in Table 6 and Figure 9.

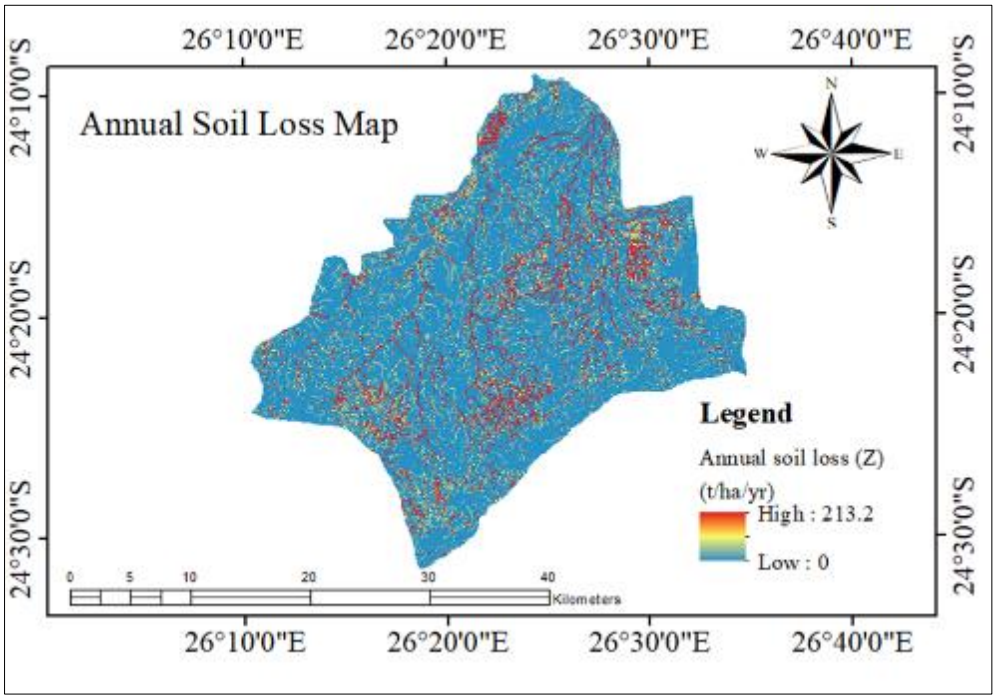

Figure 8 Spatial distribution of annual soil loss of Dinogeng Agricultural Extension Area

3.3. Potential erosion risk analysis

The study area was classified into five soil erosion risk categories shown in Figure 9 [6]. The area and proportion of soil erosion risk classes are illustrated in Table 6. The estimated soil erosion risk averaged 0.9 t ha^{-1} yr^{-1}. The maximum and minimum losses are ranging from about 0 $tha^{-1}{\cdot}yr^{-1}$ to 213.2 $tha^{-1}{\cdot}yr^{-1}$. Eighty-eight percent of the study area (69, 999 ha) has erosion risk of 0 $tha^{-1}yr^{-1}$ to 2 $tha^{-1}y^{-1}$ (low to moderate). Only 2% (1905 ha) and 10% (7946 ha) of the study area experience very high to extreme soil erosion loss rate of 5-10 $tha^{-1}yr^{-1}$ and ≥10 $tha^{-1}yr^{1}$, respectively. The spatial patterns of the estimated soil erosion risk indicate very high to extreme erosion risk areas are occurring along the streams, at steep slopes and areas of bare land. Similar studies have been done to produce soil erosion hazard maps for agricultural and management planning [8, 9, 17, 18].

Soil erodibility and topography were found to be key determinants of soil erosion risk in the study area according to SLEMSA model. However, areas with a high slope are small compared to plain and flat areas. A larger portion of the study area is located on flat areas which experience low erosion. Vegetation is a human controlled factor and thus by implementing conservation measures and preserving existing vegetation, erosion risks can be greatly reduced.

Table 6 Estimated soil erosion risk in Dinogeng Agricultural Extension Area for 2020 LULC

Erosion risk classes	Soil loss (tha-1yr-1)	Area (ha)	Percentage
Low	0 - 1	62521.0	75%
Moderate	1 - 2	7477.9	9%
High	2 - 5	3266.7	4%
Very high	5 - 10	1905.4	2%
Extremely high	>10	7946.0	10%

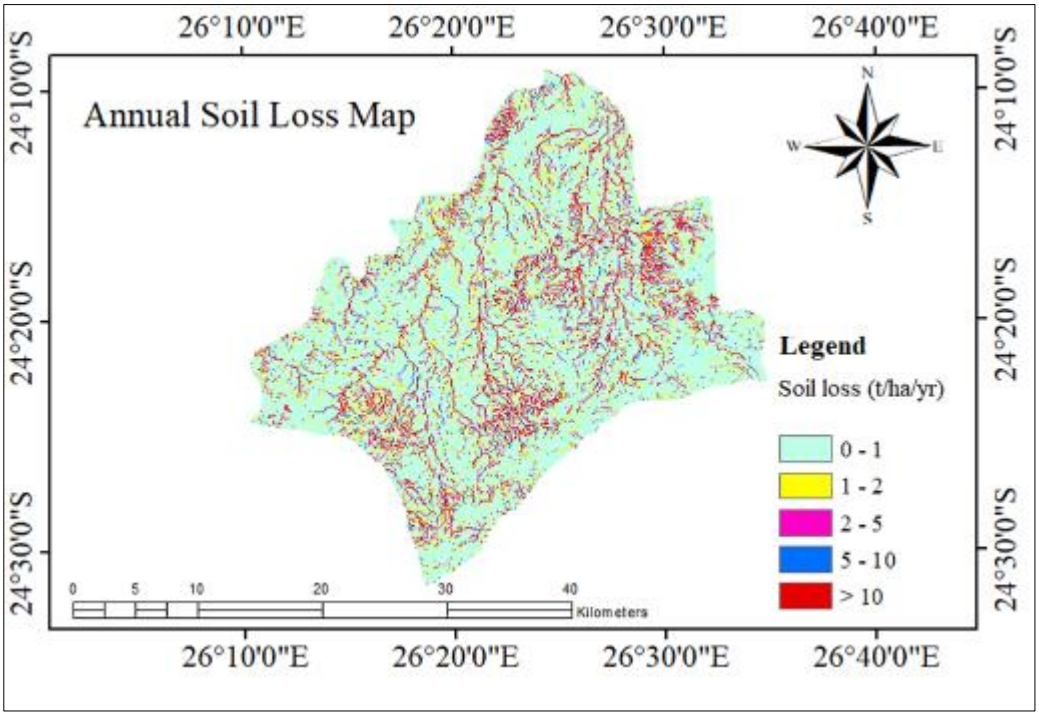

Figure 9 Soil erosion risk map for Dinogeng Agricultural Extension Area

4. Conclusion

In mapping soil erosion hazards, the integration of SLEMSA in GIS was used to estimate the spatial distribution of soil loss in the Dinogeng Agricultural Extension Area (DAEA) using the LULC map of 2020 Landsat imagery. The results

indicated that 88% of DAEA has low to moderate soil erosion risk (0 – 2 $tha^{-1}yr^{-1}$). Only 12% of the study area experience very high to extreme high erosion risk (5 - ≥10 $tha^{-1}yr^{-1}$) along the streams, at steep slopes and areas of bare land. The results of the study have shown SLEMSA as a useful model to differentiate areas of high and low erosion potential.

This study has underscored the role of topography and soil erodibility, as natural factors, in driving soil erosion. As a larger portion of the study area is located on flat areas which experience low erosion, LULC is a key human controlled factor affecting erosion, and therefore, implementing conservation measures and preserving existing vegetation can greatly reduce erosion risks.

Compliance with ethical standards

Acknowledgments

The authors are grateful to the Department of Forestry and Range Resources (DFRR) of the Ministry of Environment, Wildlife and Tourism for providing forest information for Kgatleng District from their GIS database, the Department of Meteorological Services (DMS) for availing climatic data and the United States Geological Survey (USGS) Earth Resources Observation Systems (EROS) for downloading satellite images of the study area.

Disclosure of conflict of interest

We the authors of this paper hereby declare that there are no competing interests in this publication.

References

[1] Ashiagbor G, Forkuo EK, Laari P and Aabeyir R. (2013). Modelling soil erosion using RUSLE and GIS tools. International Journal of Remote Sensing, 2(4), 7-13.

[2] Watershed for soil conservation planning in Highlands of Ethiopia. International Journal of Agricultural Research Innovation & Technology, 5 (2): 21-30.

[3] Manyiwa T and Dikinya O. (2013). Using universal soil loss equation and soil erodibility factor to assess soil erosion in Tshesebe village, north east Botswana. African Journal of Agricultural Research, 8(30), 4170-4178.

[4] Kayombo B, Meulenberg F, Moganane BG, Dikinya O, Aliwa JN, Nsinamwa M, Gaboutloeloe G, Patrick C, Mzuku M and Machacha S. (2005). Characterization of agriculture land degradation in Botswana. Botswana Journal of Technology, 14(1), 1 - 10.

[5] Bobe BW. (2004). Evaluation of Soil Erosion in the Harerge Region of Ethiopia usin soil loss models , rainfall simulation and field trials. Ph.D. thesis, University of Kwazulu Natal, South Africa, 142-168.

[6] Marondedze AK and Schütt B. (2020). Assessment of soil erosion using the RUSLE model for the Epworth District of the Harare Metropolitan Province, Zimbabwe. Sustainability, MDPI, 12(20),1-24.

[7] Vargas R and Omuto C. (2016). Soil loss Assessment in Malawi . Food and Agriculture Organization of the United Nations and the UNDP-UNEP Poverty-Environment Initiative and the Ministry of Agriculture, Irrigation and Water Development, Malawi, 30 pages.

[8] Elwell HA. (1978). Modelling soil losses in Southern Africa. Journal of Agricultural Engineering Research, 23(2), 117-127.

[9] Stocking M, Chakela Q and Elwell H. (1988). An improved methodology for erosion hazard mapping Part I : The Technique. Geografiska Annaler, 70(3), 169- 180.

[10] Heydarnejad S, Fordoei AR, Mousavi SH and Mirzaei R. (2020). Estimation of soil erosion using SLEMSA model and OWA approach in Lorestan Province (Iran). Environmental Resources Research, 8(1), 12-24.

[11] Wischmeier WH and Smith DD. (1978). Predicting Raifall Erosion Losses; A guide to Conservation Planning, USDA Handbook No. 537, 67.

[12] Morgan RPC and Davidson D. (1991). Soil erosion and conservation. Longman, UK, 276-278.

[13] Bvindi, A. (2019). Assessment of soil erosion hazard around the abandoned Nyala mine in formerly Mutale Municipality, Limpopo Province, South Africa. M.Sc. thesis, University of Kwazulu Natal, South Africa, 60-65.

[14] Hurni, H. (1985). Erosion productivity conservation systems in Ethiopia. Proceedings of 4th International Conference on Soil Conservation, Maracay, Venezuela, 3-9 November 1985, 654-674.

[15] Morgan, RPC. (1995). Soil erosion and conservation, 2nd Edition. Longman Group, UK, 256-263.

[16] Parece T, Campbell JB and McGee J. (2017). Remote Sensing Analysis in an ArcMap Environment, 2nd Edition. Independently published, 267pp.

[17] Igwe CA, Akamigbo FOR and Mbagwu JSC. (1999). Application of SLEMSA and USLE erosion models for potential erosion hazard mapping in south-eastern Nigeria. International Agrophysics, 13(1), 41-48.

[18] Shahzeidi SS, Entezari M, Gholami M and Dadashzadah Z. (2019). Assessment rate of soil erosion by GIS: Case study of Varmishgan, Iran. Journal of Basic Applied Science Research, 2(12), 13115-1312.